American Mineralogist, Volume 102, pages 1971–1976, 2017

SPECIAL COLLECTION: BIOMATERIALS—MINERALOGY MEETS MEDICINE

Substitution of sulfate in apatite

Linh K. Tran[1], Kathleen R. Stepien[1], Melissa M. Bollmeyer[1], and Claude H. Yoder[1,*]

[1]Department of Chemistry, Franklin & Marshall College, Lancaster, Pennsylvania 17604, U.S.A.

Abstract

The substitution of sulfate in apatite is of potential importance in synthetic biomaterials used in bone repair and reconstruction. The counter ion (e.g., Na^+, K^+, Mg^{2+}, Sr^{2+}) in the sulfate reagent may also be used as a source of medically beneficial ions. An understanding of the structural parameters controlling sulfate substitution is also important in expanding our knowledge beyond the substitution of carbonate in apatites.

The incorporation of sulfate in calcium and strontium hydroxylapatites, prepared in aqueous solution at pH 9, was verified by combustion analysis of sulfate, infrared and Raman spectroscopy, and by determination of unit-cell parameters. Sulfate could not be incorporated into barium hydroxylapatite because of the preferential formation of $BaSO_4$.

The amount of sulfate substituted in the apatite was affected by the mole ratio of sulfate to phosphate in the reaction mixture and by the nature of the counter ion in the sulfate reagent. When sodium is the counter ion in the sulfate reagent, the molar amounts of both sodium and sulfate in the product apatite can be explained by assuming charge compensation by sodium ions and sulfate displacement of phosphate and calcium. With lithium as the counter ion, a greater molar amount of lithium than sulfate is incorporated into the apatite, an observation that requires an additional charge-compensation mechanism. With potassium and rubidium as counter ions, less of the counter ion is incorporated than sulfate, probably a result of less favorable accommodation of the larger cation in the apatite structure.

The maximum molar amount of sulfate incorporated in hydroxylapatite (prepared in the presence of Na^+) is more than three times lower than the maximum molar amount of carbonate that can be incorporated, a difference that can be explained by the relative solubilities of the substituted apatites. The unit-cell parameters determined for both sulfated calcium and strontium hydroxylapatites synthesized with the sodium counter ion show a slight increase in the *a*-axis length and a nearly constant *c*-axis length with increasing sulfate content. The difference in the variation of unit-cell parameters with anion content can be rationalized by the difference in size of the anion.

The results indicate that sulfate can be incorporated into biomaterials such as apatite or in composites with calcium sulfate and that the design of new apatites and composites could include the use of medically desirable counter cations.

Keywords: Apatite, sulfate, incorporation of sulfate, unit cell, IR, strontium apatite, sulfated apatite, calcium sulfate-apatite composite, Biomaterials—mineralogy meets medicine

Introduction

Calcium sulfate has been used as a biomaterial since the later part of the 19th century. It has been used to repair bone defects, augment sinuses, and in various dental applications (Thomas and Puleo 2009; Ricci et al. 2000). Discussions of the mechanism by which this extraordinary compound operates usually focus on the efficacy of its resorption and its ability to initiate production of a calcium-phosphate lattice; that is, to stimulate new bone growth (Ricci et al. 2000). Increased calcium ion concentrations may act as a stimulus to osteoblasts (bone-producing cells) and inhibitor of osteoclast (bone-dissolving cells) activity (Thomas and Puleo 2009). Calcium sulfate has been combined with organic compounds such as gelatin, poly(lactic) acid, and carboxymethylcellulose, as well as calcium phosphate and hydroxylapatite [$Ca_{10}(PO_4)_6(OH)_2$, in this work designated as CaApOH]. Parsons et al. (1988) report on mixtures that are "osteoconductive composite grouts for orthopedic use." Mixtures of calcium sulfate with either apatite or calcium phosphate have been reported to resorb more slowly, which can have clinical advantages (Parsons et al. 1988; Urban et al. 2007; Fillingham et al. 2012; Yang et al. 2012; Kuo et al. 2015). Because apatite has a singular ability to accommodate ions by substitution, it is possible that the efficacy in bone healing/renewal of calcium sulfate alone and in composites together with hydroxylapatite may involve substitution of sulfate in the newly formed biological apatite. Moreover, the use of sulfated apatite (SCaApOH), rather than CaApOH, in mixtures with calcium sulfate may be advantageous.

Among the many anions that can function as substituents in apatite, carbonate has received the most attention primarily due to its presence in bones and teeth. The substitution of sulfate

* E-mail: cyoder@fandm.edu

Special collection papers can be found online at http://www.minsocam.org/MSA/AmMin/special-collections.html.

0003-004X/17/0010–1971$05.00/DOI: http://dx.doi.org/10.2138/am-2017-6088

ion, on the other hand, is poorly understood. One might anticipate that on the basis of its charge, sulfate would behave like carbonate and replace either phosphate (B-type substitution) or the monovalent ion (A-type substitution). On the other hand, its structural and electronic similarity to phosphate—sulfate and phosphate are isoelectronic—suggest that sulfate might only replace phosphate, with appropriate accommodations to maintain local charge neutrality in the apatite structure. The larger size of sulfate mitigates against its ability to substitute for monovalent anions in the apatite channels. The smaller carbonate ion, which has a volume of 28 Å^3 [as opposed to 43 Å^3 for sulfate, both calculated from thermodynamic radii (Roobottom et al. 1999)], can replace channel hydroxide to a limited extent in apatites that have estimated channel volumes of about 30 Å^3 or less (Goldenberg et al. 2015).

That sulfate can take the place of phosphate to produce compounds with an apatitic stoichiometry and structure is supported by the existence of "sulfate" apatites, such as $Na_6Ca_4(SO_4)_6F_2$, and $Na_6Pb_4(SO_4)_6F_2$ (Klement 1939; Kreidler and Hummel 1970), and compounds containing both orthosilicate and sulfate, such as $M_{10}(SiO_4)_3(SO_4)_3F_2$, where M = Ca, Sr, and Pb (Kreidler and Hummel 1970) occur naturally (ellestadite is the F/OH endmember for M = Ca, McConnell 1937; Khorari et al. 1994) and also have been synthesized. A recent study of sulfate substitution in hydroxylapatite, using microwave heating of the aqueous reaction mixture, produced a compound whose formula was given as $Ca_{10}(PO_4)_{6-x}(SO_4)_x(OH)_{2-x}$, with x = 0.05–0.5 (Alshemary et al. 2013). Evidence for the incorporation of sulfate included X-ray diffraction and IR peak broadening, as well as an increase in both the *a*- and *c*-axis lengths with increased sulfate concentration in the product. Hydrothermal processing of a mixture of sulfate and amorphous calcium phosphate produced sulfated hydroxylapatites that showed no change in lattice parameters (Toyama et al. 2013).

To explore the possible role of sulfate substitution in apatite as part of the biocompatibility and resorbability of calcium sulfate and sulfated hydroxylapatite, we report here our studies of sulfate incorporation into hydroxylapatite. Because biomaterials can be designed with ancillary ions that can provide additional nutrients (Pasteris 2016), we have also studied the effect of the counter ion in the sulfate reagent on the incorporation process. The use of selected counter ions (e.g., Li^+, Na^+, K^+, Zn^{2+}, Mg^{2+}) in the sulfate reagent may produce apatites deliberately doped with medically desirable ions that could be released during dissolution/resorption of the biomaterial. To provide greater depth of understanding about substitution processes in apatite, we also include our work on sulfate substitution in strontium and barium hydroxylapatites.

Experimental methods

Milli-Q deionized water and ACS Reagent grade reagents with purities above 98% were used for the preparation of all samples.

Syntheses

Sulfated calcium and strontium apatites were synthesized in a round bottom flask using the following solutions: 0.33 M $Ca(NO_3)_2{\cdot}4H_2O$ or 0.33 M $Sr(NO_3)_2$, 0.20 M A_2SO_4, and 0.20 M $NH_4H_2PO_4$ with A = Li, Na, K, Rb. The amounts of each solution used were based on the 5:3:1 stoichiometry of $M_5(PO_4)_3OH$ rather than the formula (vide infra) of the desired apatite. The amount of the sulfate solution was varied to provide sulfate to phosphate mole ratios of 0.5:1 up to 4:1 (sulfate:phosphate). In separate dropping funnels, the solutions of $NH_4H_2PO_4$ and $M(NO_3)_2$ were added dropwise at 0.5 drop per second to the A_2SO_4 solution, magnetically stirred in a round bottom flask at 80 °C. The pH of the mixture was adjusted to 9 with 3 M NH_3 after 10 drops of each reagent were added. The pH of the mixture was maintained at 9 during the addition and digestion periods using 3 M NH_3. After the digestion time of 24 h, during which the reaction mixture was stirred and heated, the white precipitate was suction filtered and washed 6 times using Milli-Q water. The product was dried in a vacuum oven for 24 h at 120 °C and 5 torr. The yields were 85–95%.

Identification and analysis

All products were identified by X-ray diffraction using a PANalytical X'Pert PRO Multi purpose diffractometer Theta-Theta System with Cu*K*α radiation (λ = 1.54060 Å) and analyzed using the PANalytical program X'Pert Highscore Plus. Samples were prepared on a 32 mm glass slide for scanning (30 min) with a range from 5 to 70° 2θ.

IR spectra were obtained on a Bruker Tensor 37 IR Spectrometer with a Ge ATR mount using 256 scans and a resolution of 2 cm^{-1}.

In addition to combustion analysis of sulfur (Galbraith Laboratories, Knoxville, Tennessee, and in-house use of a Costech ECS 4010 CHNS-O system), the presence of sulfate in each apatite sample was confirmed by precipitation of $BaSO_4$ from an acid solution (3 M HNO_3) of the sulfated apatite.

The weight percent of metal ions, phosphorus, and sulfur were obtained using a SPECTRO Analytical ICP-AES SPECTROBLUE spectrometer [wavelengths (nm): Ca = 422.673, P = 177.495, Na = 589.592, Li = 670.780, K = 769.896, S = 182.034]. Calibration curves were prepared by dilution of commercial standards of Ca, K, Na, Li, S, and P (1000 ppm) with 8 M HNO_3. Apatites were dissolved in 8 M HNO_3 solution before analysis. The errors in all elemental data are expected to be no greater than 5%.

Elemental composition was also obtained using X-ray fluorescence spectroscopy with a PANalytical PW 2404 Vacuum Spectrometer equipped with a 4kW Rh X-ray tube. Sample preparation involved ignition to 1200 °C to create an anhydrous powder, followed by preparation of glass disks using nine parts lithium tetraborate and one part anhydrous sample material.

Unit-cell parameters were determined from 2.5 h XRD scans of samples. Peaks were indexed following a star-quality PDF card that matched the experimental pattern with the highest score. The program UnitCell for OS X (Holland and Redfern 1997) provided an initial set of *a*- and *c*-axis values that were refined by eliminating potentially deleterious peaks. Unit-cell parameters were also determined with the PANalytical X'pert Highscore Plus (ver. 2.3e) program. Based on repeated determinations of unit-cell parameters on one compound the error is estimated to be ±0.001 Å. The two methods produced cell parameters generally within ±0.001 Å.

Results and discussion

Synthesis

Sulfated calcium and strontium hydroxylapatites were prepared by aqueous addition of reagents containing lithium, sodium, potassium, and rubidium as the sulfate counter ion. The reaction of sodium sulfate with calcium nitrate and ammonium dihydrogen phosphate produced sulfated calcium hydroxylapatites (SCaApOH) containing 2 to 8 wt% sulfate. The relationship between the weight percent sulfate in the apatite and the mole ratio of sulfate to phosphate used in the reaction mixture is shown in Figure 1, which indicates saturation of the apatite structure with sulfate at about 8 wt% (with sodium as the sulfate counter ion). $CaSO_4$ (gypsum) was detected by Raman spectroscopy in reactions that utilized a 4:1 mole ratio of sodium sulfate to phosphate: at this mole ratio formation of the slightly insoluble $CaSO_4$ becomes competitive with continued incorporation of sulfate.

By contrast, the maximum weight percent carbonate incorporated in calcium hydroxylapatites is about 17% (Pasteris et al. 2014) (22.5% was reported by LeGeros et al. 1967), indicating that a significantly greater number of moles of carbonate can be incorporated in the structure. This difference in the amount of

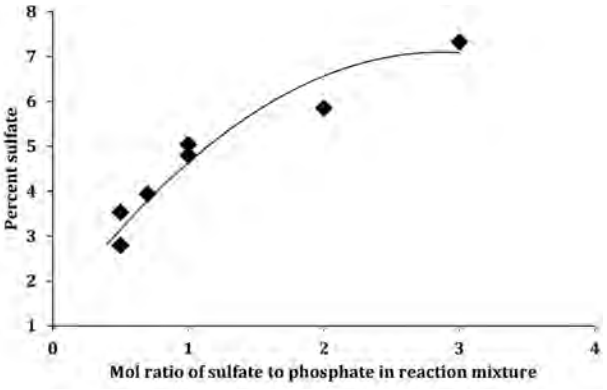

FIGURE 1. The wt% sulfate incorporated into CaApOH as a function of the mole ratio of sulfate to phosphate in the reaction mixture with sodium as counter ion.

anion incorporated can be attributed to the greater insolubility of carbonated apatite relative to sulfated apatite, as rationalized using the simple salt approximation for the solubility of double salts (Yoder and Rowand 2006).

Sulfated strontium hydroxylapatites were prepared analogously, but the formation of $SrSO_4$ was observed at mole ratios (sulfate:phosphate) of 0.4:1 and higher. The use of mole ratios of 0.1:1 up to 0.4:1 produced sulfated strontium hydroxylapatite with sulfate weight percentages ranging from 1.2 to 2.2 (and no $SrSO_4$ detectable by XRD). Attempts to prepare sulfated barium hydroxylapatites (SBaApOH) lead to the formation of $BaSO_4$, even at a mole ratio of 0.1:1. The change in the amount of sulfate incorporated in the alkaline earth apatites is likely due primarily to the decrease in solubility of the sulfate salts (K_{sp} $CaSO_4$, 10^{-5}; $SrSO_4$, 10^{-7}; $BaSO_4$, 10^{-10}), which are formed in the reaction mixtures.

Composition

Powder X-ray diffraction patterns of the sulfated apatites (SCaApOH) were in good agreement with the pattern for CaApOH (PDF 98-002-2060) and showed no appreciable change in line widths with increased incorporation of sulfate. The wt% Na and SO_4 of selected calcium hydroxylapatites prepared with sodium sulfate present in the reaction mixture are shown in Table 1. The samples are arranged in order of increasing wt% SO_4, and it is clear that the wt% Na increases in the same order. Indeed, the number of moles of sodium is roughly the same as that of sulfate. Thus, the incorporation of sulfate is accompanied by the incorporation of sodium.

A formula for the sulfated hydroxylapatites may be determined from the relationship between the number of moles of calcium and sulfate and the number of moles of alkali metal counter ions in each of the hydroxylapatites. These relationships appear in Figures 2 and 3. Figure 2 shows an inverse 1-to-1 relationship between calcium and sulfate ions: substitution of sulfate is accompanied by a loss of calcium ions. With the number of moles of calcium normalized to 10 for the compound with 0 mol of sulfate [where the formula of the compound should be $Ca_{10}(PO_4)_6(OH)_2$] the intersection of the extrapolated line in Figure 2 with the x-axis suggests that a limiting sulfated hydroxylapatite prepared with sodium as the counter ion may contain three moles of sulfate and 7 mol of calcium.

Figure 3 shows the relationship between moles of sulfate and the moles of alkali metal counter ion (present in the sulfate reactant) incorporated. This reactant in most cases was Na_2SO_4, but in five reactions Li_2SO_4 was used, and in five K_2SO_4 was one of the reactants (Rb_2SO_4 was also employed to confirm observations, vide infra). It is well known that Na^+ can be incorporated into the apatite lattice. Limited substitution of Li, Na, and K for calcium has been reported (Simpson 1968; Mayer et al. 1986; Fleet and Liu 2007; Whyte et al. 2008; Zyman and Tkachenko 2013; Yoder et al. 2016).

TABLE 1. Weight percent of sodium and sulfate in selected sulfated calcium hydroxylapatites prepared using sodium sulfate

Sample	wt% Na	wt% SO_4
1	0.02	0.04
2	0.07	1.69
3	0.93	2.79
4	1.13	3.90
5	1.22	4.19
6	1.68	5.51
7	1.95	6.47

Charge compensation

The presence of the counter ion in the apatite structure, presumably as replacements for some of the Ca(2) cations in the apatite channel (Pan and Fleet, 2002), is to be expected given the charge compensation necessary for substitution of a –2 anion

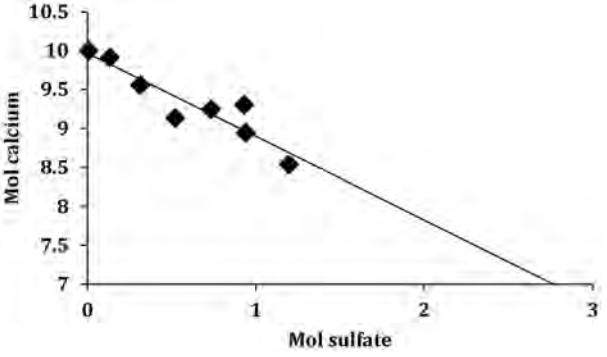

FIGURE 2. Relationship between calcium content and amount of sulfate incorporated in calcium hydroxylapatites with sodium as counter ion.

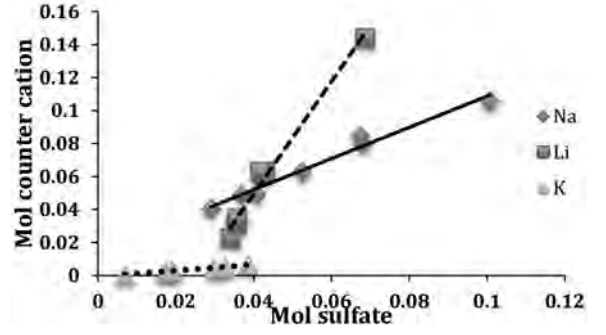

FIGURE 3. Relationship between sulfate and counter cation content. Squares = Li, diamonds = Na, triangles = K.

(SO_4^{2-}) for a –3 anion (PO_4^{3-}). De Maeyer et al. (1996) provide six fundamental substitution schemes for carbonate substitution, of which five are pertinent to B-type substitution. These are rewritten below for sulfate substitution and without designation of vacancies (M represents the counter ion):

(1) $SO_4^{2-} \rightarrow PO_4^{3-} + Ca^{2+} + OH^-$;
(2) $2\ SO_4^{2-} \rightarrow 2\ PO_4^{3-} + Ca^{2+}$;
(3) $SO_4^{2-} + M^+ \rightarrow PO_4^{3-} + Ca^{2+}$;
(4) $M^+ \rightarrow Ca^{2+} + OH^-$;
(5) $SO_4^{2-} + OH^- \rightarrow PO_4^{3-}$.

Although our reactions were carried out at pH 9, scheme 5 is probably not likely and was not observed in the extensive study of De Maeyer et al. (1996). De Maeyer et al. (1996) found that schemes 1 and 2 were predominantly employed in their synthetic methods using sodium and potassium salts to synthesize carbonated apatites. It is important to realize that the charge compensation scheme used during the synthesis depends on the reagents and conditions. The stoichiometry of the product apatite also may be best explained by a combination of charge compensation schemes.

Interestingly, each of the alkali metal cations has its own relationship (Fig. 3) to sulfate content, with the lines for all three counter ions extrapolating to close to zero at 0 mol of sulfate. The slopes of the lines are very different, presumably a result of a change in charge compensation mechanism and/or stereostructural constraints. The relationship between moles of counter ion and moles of SO_4^{2-} incorporated is approximately 1-to-1 for Na^+, less than 1 for K^+, and greater than 1 for Li^+. In other words, the incorporation of, say, 0.05 mol of sulfate is accompanied by the incorporation of roughly the same amount of Na^+, about 0.01 mol of K^+, and almost 0.1 mol of Li^+.

The charge-balance mechanism for the sulfated hydroxylapatites made with sodium as the counter ion is therefore almost surely the replacement of one calcium ion by one sodium ion (scheme 3):

$$SO_4^{2-} + Na^+ = PO_4^{3-} + Ca^{2+}.$$

This relationship is similar to that found by Montel et al. (1981) for carbonated hydroxylapatites. Thus, the formula of the sulfated hydroxylapatites precipitated in the presence of sodium ion can be written as $Ca_{10-x}(Na)_x(PO_4)_{6-x}(SO_4)_x(OH)_2$, where x = moles sulfate. For the limiting apatite containing 3 mol of sulfate (vide supra), the formula is $Ca_7Na_3(PO_4)_3(SO_4)_3(OH)_2$, which contains 30% sulfate and cannot be prepared using our experimental procedure.

Because the sulfated hydroxylapatites prepared using lithium sulfate contain more than twice as much lithium as sulfate, the charge-balance mechanism cannot be expressed using only schemes 1, 2, or 3. The addition of scheme 4, the independent incorporation of Li^+, is necessary and also requires removal of calcium and hydroxide ions.

$$M^+ \rightarrow Ca^{2+} + OH^- \quad (4)$$

Enhanced uptake of lithium in the synthesis of carbonated apatites was also reported by Mayer et al. (1986). In the IR spectra (Fig. 4) of the lithium sulfate incorporated apatites, the OH peak at 3570 cm^{-1} decreases as the amount of sulfate increases, consistent with the operation of schemes 1 or 4.

For those apatites sulfated using K_2SO_4, considerably less K^+ is present than required by scheme 3. For these compounds most of the sulfate incorporation occurs via scheme 1 or 2. The small amount of potassium in the sulfated apatites is contrary to the composition of carbonated apatites containing potassium prepared at high temperatures where the mole ratio of potassium and carbonate is close to 1-to-1 (Verbeeck et al. 1995). It is also clear from Figure 3 that the amount of sulfate incorporated when the counter ion is potassium is two to three times smaller than the amount incorporated with Na as counter ion. Thus, some sulfate may be incorporated with simultaneous incorporation of potassium (scheme 3), but most of the sulfate enters through the operation of schemes 1 or 2. Because the total amount of sulfate is low, this observation indicates that the use of scheme 1 or 2 contributes a smaller amount to charge-compensation than does scheme 3 when lithium and sodium are the counter ions.

The relatively minor incorporation of K^+ suggests that larger cations may not easily be incorporated into the apatite structure. This observation is supported by the even smaller molar amounts of rubidium found in SCaApOH prepared using Rb_2SO_4. For the apatite prepared using the largest mole ratio of 3:1 (sulfate:phosphate) only 0.04 wt% Rb was found compared to 0.2 wt% K in an apatite prepared using a similar mole ratio (this corresponds to the incorporation of about a tenth as many moles of Rb as K). It is worth noting that the molar amount of alkali metal ions incorporated follows the trend $Li^+ > Na^+ > K^+ > Rb^+$, which is the inverse order of their sixfold-coordinated ionic radii. Both K^+ (1.38 Å) and Rb^+ (1.52 Å) are significantly larger than Ca^{2+} (1.00 Å).

IR and Raman spectra

The presence of incorporated sulfate in both CaApOH and SrApOH samples was confirmed by IR and Raman spectra. The Raman spectrum of SSrApOH containing 4 wt% sulfate contains a peak at 1004 cm^{-1}, consistent with the sulfate symmetric stretching (ν_1) peak at 1008 cm^{-1} in gypsum, as well as a peak at 3570 cm^{-1} for the OH stretch (Fig. 5). These assignments are consistent with those of Pasteris et al. (2014) for the OH stretch and Liu et al. (2009) for the symmetric sulfate (ν_1) stretching mode. IR spectra for four SCaApOH samples prepared using various mole ratios of sulfate to phosphate show an increase in the asymmetric sulfate stretching (ν_3) peak intensity at ca. 1100 cm^{-1} consistent with an increase in sulfate content (Fig. 6).

Unit-cell parameters

Additional evidence for the incorporation of sulfate into the apatite structure comes from the relationship between wt% sulfate and the unit-cell axial lengths (Fig. 7). The increase in the *a*-axis length over a range of 2 wt% sulfate is about 0.015 Å. The increase in *a*-axis length is not consistent with the thermodynamic radius of sulfate (2.18 Å, Roobottom et al. 1999) relative to that of phosphate (2.47 Å, derived from the apatite-appropriate volume of 0.063 nm^3, Flora et al. 2004) but is consistent with Dasent's values (Dasent 1982) of 2.58 Å for sulfate and 2.38 Å for phosphate as well as the ion volumes of 0.091 nm^3 for sulfate (Marcus et al. 2002) and 0.063 nm^3 for phosphate (Flora et al. 2004). An increase in *a*-axis length (as well as the *c*-axis length) was also observed by Alshem-

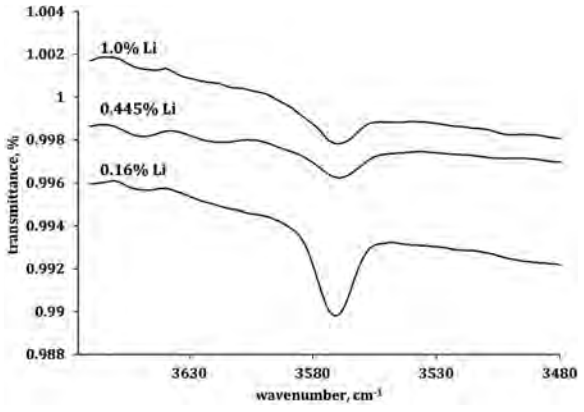

FIGURE 4. The OH region of the IR spectra of several SCaApOH apatites prepared using lithium as the counter ion. Spectra normalized to the ν_3 phosphate band.

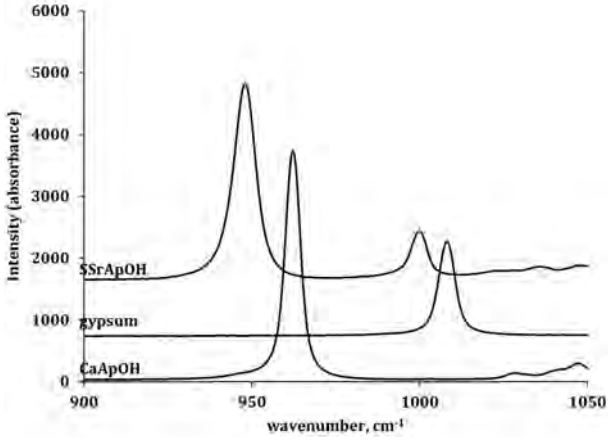

FIGURE 5. The Raman spectra of the phosphate and sulfate stretching regions of (top) SSrApOH showing the ν_1 phosphate stretch at 948 cm^{-1} and the ν_1 sulfate stretch at 1000 cm^{-1}, (middle) gypsum (1008 cm^{-1}), and (bottom) non-sulfated CaApOH (Sigma-Aldrich).

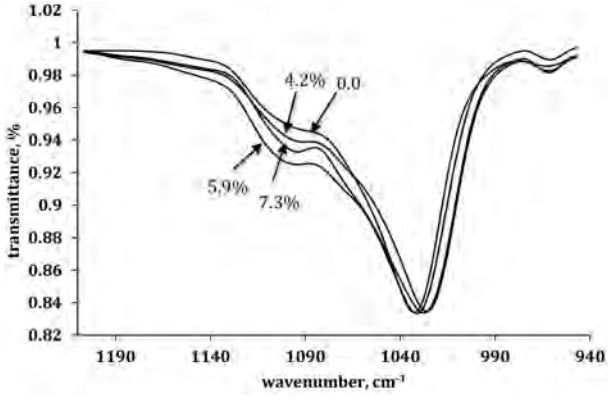

FIGURE 6. The 960 to 1200 cm^{-1} region of the IR spectra in SCaApOH samples containing varying amounts of sulfate. The peak at 1030 cm^{-1} is the ν_3 P-O stretching band; the peak at ca. 1100 cm^{-1} is the ν_3 S-O stretching band.

ary et al. (2013), whereas Toyama et al. (2013) found no change in axial lengths.

The variation in axial lengths was also determined for a series of sulfated strontium hydroxylapatites using four samples prepared with Na_2SO_4 at low mole ratios (0.1:1 up to 0.4:1) and two obtained at higher mole ratios where $SrSO_4$ was also present as a separate phase. These axial lengths (Fig. 8) show the same increase in *a*-axis with percent sulfate observed for the calcium analogs (Fig. 7).

IMPLICATIONS

Our study reveals that sulfate can be incorporated into CaApOH, and that while lattice parameters for the sulfated apatites are similar to those of CaApOH, the *a*-axis length increases with an increase in wt% sulfate.

Such incorporation of sulfate into CaApOH, and its measurement, is important for several reasons. Because of the recognition of therapeutic properties of calcium sulfate in bone healing and reconstruction, it is reasonable to assume that the incorporation of sulfate in apatite should be explored in creating new biomaterials using sulfated calcium apatite alone or in a composite with calcium sulfate. Sulfation of apatite may also be involved in creating new bone material using calcium sulfate and calcium sulfate-phosphate/

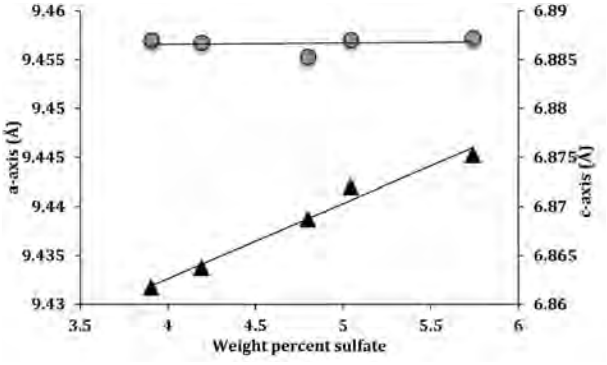

FIGURE 7. The effect of incorporated sulfate on the unit-cell *a*- and *c*-axial lengths for SCaApOH synthesized using sodium as the counter ion. The *a*-axis is represented by triangles and the *c*-axis by circles.

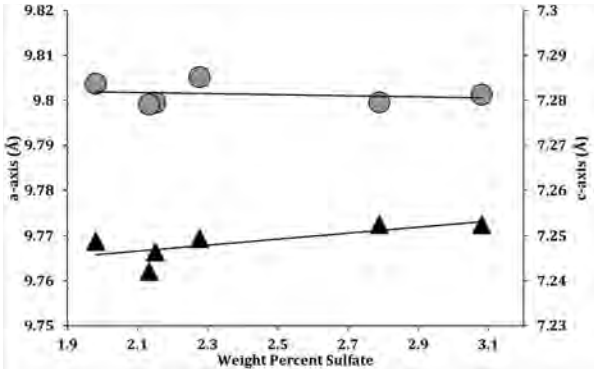

FIGURE 8. Variation of unit-cell axial lengths with sulfate percentage for SSrApOH. The *a*-axis is represented by triangles and the *c*-axis by circles.

apatite composites.

Because the counter ion of the sulfate reagent is incorporated into apatite, to an extent dependent on ionic radius and the cocentration ratio of reagent to phosphate, ions present in the sulfate reactant can be tailored to produce beneficial effects on bone mineral (LeGeros et al. 2009; Shepherd et al. 2012). Substituted apatites generally have a greater solubility in water than the parent apatite, potentially increasing their resorbability and biocompatibility.

Although the solubility of sulfated apatite in water has not yet been determined, it is likely that sulfated apatite is more soluble than carbonated apatite (Yoder and Rowand 2006), but contains a substituent (the sulfate ion) that is the conjugate base of a strong acid, whereas carbonate is the conjugate base of a weak acid. This difference in basicity of the substituent ion may affect the solubility of the substituted apatite as a function of pH, which is likely to be related to bioresorption of apatite (Arnett 2008).

More generally, our work shows that the extent of sulfation (and, perhaps, most substitutions in the apatite structure) depends upon the nature of the counter ion in the sulfate reactant. We also suggest that the size of the substituent determines the type of substitution (A- vs. B-type) and the relative solubilities of the substituted apatite (SCaApOH vs. CCaApOH).

Acknowledgments

The authors are indebted to the Camille and Henry Dreyfus Foundation for a Senior Scientist Mentor award (C.H.Y.) and to the Lucille and William Hackman Program at Franklin & Marshall College for funding. This material is based upon work supported by the National Science Foundation under Grant No. 0923224. The authors gratefully acknowledge helpful conversations and the acquisition of Raman spectra by Jill D. Pasteris at Washington University, St. Louis, Missouri, and sulfur analyses by Karen Mertzman and XRF analyses by Stanley Mertzman at Franklin & Marshall College.

References cited

Alshemary, A.Z., Goh, Y-F., Akram, M., Razali, I.R., Kadir, M.R.A., and Hussain, R. (2013) Microwave assisted synthesis of nano-sized sulphate doped hydroxyapatite. Materials Research Bulletin, 48, 2106–2110.

Arnett, T.R. (2008) Extracellular pH regulates bone cell function. The Journal of Nutrition, 138, 4155–4185.

Dasent, W.E. (1982) Inorganic Energetics, 2nd ed. Cambridge University Press, New York.

De Maeyer, E.A.P., Berbeeck, R.M.H., and Pieters, I.Y. (1996) Carbonate and alkalimetal incorporation in calciumhydroxyapatite. Trends in Inorganic Chemistry, 4, 157–171.

Fillingham, Y.A., Lenart, B.A., and Gitelis, S. (2012) Function after injection of benign bone lesions with a bioceramic. Clinical Orthopaedics and Related Research, 470, 2014–2020.

Fleet, M.E., and Liu, X. (2007) Coupled substitution of type A and B carbonate in sodium-bearing apatite. Biomaterials, 28, 916–926.

Flora, N.J., Yoder, C.H., and Jenkins, H.D.B. (2004) Lattice energies of apatites and the estimation of $\Delta H^0_f(PO^{3-}_4,g)$. Inorganic Chemistry, 43, 2340–2345.

Goldenberg, J.E., Wilt, Z., Schermerhorn, D.V., Pasteris, J.D., and Yoder, C.H. (2015) Structural effects on incorporated water in carbonated apatites. American Mineralogist, 100, 274–280.

Holland, T.J.B., and Redfern, S.A.T. (1997) Unit cell refinement from powder diffraction data: the use of regression diagnostics. Mineralogical Magazine, 61, 65–77.

Khorari, S., Cahay, R., Rulmont, A., and Tarte, P. (1994) The coupled isomorphic substitution $2(PO_4)^{3-} \rightarrow (SO_4)^{2-} + (SiO_4)^{4-}$ in synthetic apatite $Ca_{10}(PO_4)_6F_2$: a study by X-ray diffraction and vibrational spectroscopy. European Journal of Solid State Inorganic Chemistry, 31, 921–934.

Klement, R. (1939) Natrium-Calcium-sulfatapatit $Na_6Ca_4(SO_4)_6F_2$. Naturwissenschaften, 27, 568.

Kreidler, E.R., and Hummel, F.A. (1970) The crystal chemistry of apatite: structure fields of fluor- and chlorapatite. American Mineralogist, 55, 170–184.

Kuo, T.F., Lee, S.Y., Wu, H.D., Porna, M., Wu, Y.W., and Yang, J.C. (2015) An in vivo swine study for xeno-grafts of calcium sulfate-based bone grafts with human dental pulp stem cells (hDPSCs). Materials Science and Engineering C. Materials of Biological Applications, 10, 19–23.

LeGeros, R.Z., Trautz, O.R., LeGeros, J.P., Klein, E., and Shirra, W.P. (1967) Apatite crystallites: effects of carbonate on morphology. Science, 155, 1409–1411.

LeGeros, R.Q., Ito, A., Ishikawa, K., Sakae, R., and LeGeros, J.P. (2009) Fundamentals of hydroxyapate and related calcium phosphates. In B. Basu, D. Katii, and A. Kumar, Eds., Advanced Biomaterials: Fundamentals, Processing, and Applications, p. 19–52, Wiley, New York.

Liu, Y., Wang, A., and Freeman, J.J. (2009) Raman, MIR, and NIR spectroscopic study of calcium sulfates: gypsum, bassanite, and anhydrite, 40th Lunar and Planetary Science Conference, 2128.

Marcus, Y., Jenkins, H.D.B., and Glasser, L. (2002) Ion volumes: a comparison. Journal of the Chemical Society, Dalton Transaction, 3795–3798.

Mayer, I., Berger, U., Markitziu, A., and Gedalia, I. (1986) The uptake of lithium ions by synthetic carbonated hydroxyapatite. Calcified Tissue International, 38, 293–295.

McConnell, D. (1937) The substitution of SiO^{4-}_4 and SO^{2-}_4 groups for PO^{3-}_4 groups in the apatite structure; ellestadite, the end-member. American Mineralogist, 22, 977–986.

Montel, G., Bonel, G., Heughebaert, J.C., Trombe, J.C., and Rey, C. (1981) New concepts in the comoposition, crystallization and growth of the mineral component of calcified tissues. Journal of Crystal Growth, 53, 74–99.

Pan, Y., and Fleet, M.E. (2002) Compositions of the apatite-group minerals: substitution mechanisms and controlling factors. Reviews in Mineralogy and Geochemistry, 48, 13–49.

Parsons, J.R., Ricci, J.L., Alexander, H.J., and Bajpai, P.K. (1988) Osteoconductive composite grouts for orthopedic use. Annals of the New York Academy of Sciences, 100B, 1911–1921.

Pasteris, J.D. (2016) A mineralogical view of apatitic biomaterials. American Mineralogist, 101, 2594–2610.

Pasteris, J.D., Yoder, C.H., and Wopenka, B. (2014) Molecular water in nominally unhydrated carbonated hydroxylapatite: The key to a better understanding of bone mineral. American Mineralogist, 99, 16–27.

Ricci, J.L., Alexander, H., Nadkarni, P., Hawkins, M., Turner, J., Rosenblum, S., Brezenoff, L., DeLeonardis, D., and Pecora, G. (2000) Biological mechanisms of calcium-sulfate replacement by bone. In J.E. Davies, Ed., Bone Engineering, Toronto, EM2 Inc., p. 332–344.

Roobottom, H.K., Jenkins, H.D.B., Passmore, J., and Glasser, L. (1999) Thermochemical radii of complex ions. Journal of Chemical Education, 76, 1570–1573.

Shepherd, J.H., Shepherd, D.V., and Best, S.M. (2012) Substituted hydroxyapatites for bone repair. Journal of Materials Science Materials in Medicine, 23, 2335–2347.

Simpson, D.R. (1968) Substitutions in apatite: I. Potassium-bearing apatite. American Mineralogist, 53, 432–444.

Thomas, M.V., and Puleo, D.A. (2009) Calcium sulfate: Properties and clinical applications. Journal of Biomedical Materials research Part B, 88B, 597–610.

Toyama, T., Kameda, S., and Nichimiya, N. (2013) Synthesis of sulfate-ion-substituted hydroxyapatite from amorphous calcium phosphate. Bioceramics Development and Applications, S1:011, doi: 10.4172/2090-5025.S1-011.

Urban, R.M., Turner, T.M., Hall, D.J., Inoue, N., and Gitelis, S. (2007) Increased bone formation using a calcium sulfate and calcium phosphate composite graft. Clinical Orthopaedics and Related Research, 459, 110–117.

Verbeeck, R.M.H., De Maeyer, E.A.P., and Driessens, F.C.M. (1995) Stoichiometry of potassium- and carbonate-containing apatites synthesized by solid state reactions. Inorganic Chemistry, 34, 2084–2088.

Whyte, J., Hadden, D.J., Gibson, I.R., and Skakle, J.M.S. (2008) Synthesis and stability of potassium/carbonate co-substituted hydroxyapatites. Key Engineering Materials, 361-363, 207–210.

Yang, H.L., Zhu, X.S., Chen, L., Chen, C.M., Mangham, D.C., Coulton, L.A., and Aiken, S.S. (2012) Bone healing response to a synthetic calcium sulfate/tricalcium phosphate graft material in a sheep vertebral body defect model. Biomedical Material Research B. Applied Biomaterials, 100B, 1911–1921.

Yoder, C.H., and Rowand, J.P. (2006) Application of the simple salt lattice energy approximation to the solubility of minerals. American Mineralogist, 91, 747–752.

Yoder, C.H., Landes, N.R., Tran, L.K., Smith, A.K, and Pasteris, J.D. (2016) The relative stabilities of A- and B-type carbonate substitution in apatites synthesized in aqueous solution, Mineralogical Magazine, 80, 977–983, doi: 10.1180/minmag.2016.080.035.

Zyman, Z.Z., and Tkachenko, M.V. (2013) Sodium-carbonate co-substituted hydroxyapatite ceramics. Processing and Application of Ceramics, 7, 153–157.

Manuscript received January 24, 2017
Manuscript accepted June 6, 2017
Manuscript handled by Robert Heimann